# Copper selenide film electrodes prepared by combined electrochemical/chemical bath depositions with high photo-electrochemical conversion efficiency and stability

Ahed Zyoud [a], Khaled Murtada [a], Hansang Kwon [b], Hyun-Jong Choi [c], Tae Woo Kim [c], Mohammed H.S. Helal [d], Maryam Faroun [e], Heba Bsharat [f], DaeHoon Park [g], Hikmat S. Hilal [a, *]

[a] SSERL, Chemistry, An-Najah National University, Nablus, Palestine
[b] Department of Materials System Engineering, Pukyong National University, 365 Sinseonro, Namgu, 608-739, Busan, Republic of Korea
[c] Energy Materials Laboratory, Korea Institute of Energy Research, 152 Gajeong-Ro, Yuseong-Gu, Daejeon City 34129, Republic of Korea
[d] Department of Electrical & Computer Engineering, NCTU, (ED111) 1001 Ta Hsueh Road, Hsinchu 30010, Taiwan, ROC
[e] Al-Quds University, Abu Dies-Al-Quds, Palestine
[f] Department of Physics and Engineering Physics, College of Arts and Science, University of Saskatchewan, 116 Science Place, Saskatoon S7N 5E2, Canada
[g] Sutaek-Dong 1f, 50, Gyeongchun-Ro 276Beon-gil, Guri-Si, Gyeonggi-Do, Republic of Korea

## ARTICLE INFO

## ABSTRACT

Copper selenide (of the type $Cu_{2-x}Se$) film electrodes, prepared by combined electrochemical (ECD) followed by chemical bath deposition (CBD), may yield high photo-electrochemical (PEC) conversion efficiency (~14.6%) with no further treatment. The new ECD/CBD-copper selenide film electrodes show enhanced PEC characteristics and exhibit high stability under PEC conditions, compared to the ECD or the CBD films deposited separately. The electrodes combine the advantages of both ECD-copper selenide electrodes (in terms of good adherence to FTO surface and high surface uniformity) and CBD-copper selenide electrodes (suitable film thickness). Effect of annealing temperature, on the ECD/CBD film electrode composition and efficiency, is discussed.

© 2017 Elsevier Masson SAS. All rights reserved.

## 1. Introduction

Photovoltaic (PV) devices, based on homo-junctions and tandem cells, now exhibit high conversion efficiency values of 30% or higher [1]. Despite that, PV systems demand high manufacturing costs and special preparation conditions. Thin film electrodes are emerging as alternative to the costly p-n junction (PV) systems [2—4]. Photo-electrochemical (PEC) processes based on polycrystalline metal chalcogenide (MX, where M = Zn, Cd or Cu; X = S, Se or Te) electrodes are being considered, due to their ease of preparation, low thickness, economic demand for starting chemical amounts and low environmental impact [5,6]. However, such film electrodes, based on polycrystalline MX materials, suffer serious

shortcomings, namely their poor conversion efficiencies and low stabilities. In recent reports, $Cu_2Te$ films show a maximum conversion efficiency of 5.35% while CuSe films show 4.94% conversion efficiency [7—9]. In another recent review, CdSe film electrodes exhibit only 1.6% conversion efficiency [10]. Low stability under PEC conditions is also observed for MX film electrodes [11]. The expected conversion efficiency for pristine thin film electrodes for 2020, based on US-DOE announcements, is less than 15%. Enhancing efficiency and stability of such film electrodes is thus imperative [12].

With a band gap range 2.1—2.3 eV and high absorptivity, copper selenide film electrodes are promising candidates for PEC purposes [13]. Such films have been investigated, but their PEC behavior has not been widely reported in their pristine form. Unlike their mixed ternary and quaternary systems [14], which show conversion efficiency values higher than 15%, the pristine systems show only low conversion values, vide supra. For example, copper selenide films

---

prepared by chemical bath deposition (CBD) showed relatively low conversion efficiencies [2,15]. Electrochemically deposited (ECD) CuSe film electrodes have not been widely reported for PEC purposes, presumably due to their thickness limitations.

In a recent report, both conversion efficiency and stability of CuSe film electrodes have been enhanced by coating them with electro-active materials embedded inside polymeric matrices. Conversion efficiency and stability have been enhanced due to charge transfer catalytic behavior of the electro-active materials. The untreated (pristine) CuSe films showed only 1.2% efficiency [16].

This work aims at preparing copper selenide film electrodes with relatively high PEC efficiency and stability, with no additional treatment. The technique involves a combination of the two known simple ECD and CBD methods together to yield ECD/CBD film electrodes. Both ECD and CBD methods are non-costly, facile and demand no advanced techniques of ultra-high vacuum. Such a combined technique has been successfully described here for CdSe [17] and for CdS films [3]. In this technique, a thin uniform layer is deposited onto conducting glass/FTO substrates by ECD, followed by a thicker film deposition by CBD. The resulting ECD/CBD-CuSe film is assumed to combine the advantages of both ECD and CBD preparations together. While the ECD method yields highly uniform films of good contact with the FTO surface [18], the CBD method yields films with higher thicknesses that are more suitable for PEC purposes [19—21] but have the shortcoming of lower adherence to the substrate surface [22]. Earlier ECD/CBD-CdS film electrode showed efficiency value of 0.29% [3] compared to 0.049% observed for their CBD counterpart [23]. The ECD/CBD-CdSe film exhibited ~4.4% efficiency even with no additional treatment [17] compared to 0.8% for the CBD counterpart [24]. The main goal of this work is to check if pristine ECD/CBD-copper selenide film electrodes exhibit enhancement in their PEC efficiency compared to films prepared by either ECD or CBD separately, for the first time. The strategy is to reach conversion efficiency values, of ~15%, which have recently been reported for coated copper selenide film electrodes [25], without the necessity of any further electrode treatments described earlier [26—28]. The as-deposited film performance enhancement is thus the major goal to start with in this work. The as-prepared ECD/CBD films will be prepared, characterized and examined in PEC processes, without being annealed. For comparison purposes, samples will be annealed at relatively high (250 °C) just to check for any annealing effect at this stage. Effect of annealing on film composition, surface morphology and PEC efficiency will be assessed here. Future study will follow on the ECD/CBD systems, to study the effect of annealing at a wide range of temperatures, together with effect of coating by electro-active species.

## 2. Experimental

### 2.1. Starting materials

All starting materials were purchased from Merck, Fluka or Aldrich in pure form. FTO/glass substrates (Aldrich) were highly transparent (80%) for radiations with longer than 330 nm. The substrate resistivity was ~7.0 $\Omega$/sq.

The $Na_2SeSO_3$ (source for Se ions) was prepared as described in literature [22]. $Na_2SO_3$ (20.00 g) and selenium powder (2.00 g) were added to distilled water (100 mL). The mixture was continuously stirred for 10 h at 80 °C. The mixture was then filtered and the $Na_2SeSO_3$ solution was carefully stored in a stoppered bottle in the dark.

### 2.2. Equipment

Solid state electronic absorption (EA) spectra (200—800 nm

range) were measured for different CuSe films using a Schimadzu UV-1601 spectrophotometer. For photoluminescence (PL) spectral measurement, a Perkin-Elmer LS 50 spectrometer was used with excitation wavelength 383 nm while excluding all 400 nm (and shorter) wavelengths from the detector. Atomic force microscopy (AFM) was performed on a tapping mode system equipped with a WSxM software (Nanotech Electronica, Spain), at Al-Quds University-AbuDies. Non-conductive rectangular $Si_3N_4$ cantilevers (NSG10, NT MDT Co.) having spring constants 55.5—22.5 N/m and reference frequency range 190—325 kHz were used.

Scanning electronic micrographs (SEM) and electron dispersion X-ray (EDX) spectra were measured on a Hitachi Model S-4300 Field Emission Scanning Electron Microscope in Korean Institute of Energy Research, Korea. X-ray diffraction (XRD) patterns were measured on PANalytical X'Pert PRO X-ray diffractometer using a CuKa source ($\lambda = 1.5418$ Å) at Pukyong National University, Korea. A PAR 263A Potentiostat/Galvanostat was used to measure current density v. potential (*J-V*) plots.

### 2.3. Film preparation

All FTO/glass substrates ($4 \times 1$ cm$^2$) were pre-cleaned by a washing-up detergent and distilled water, followed by soaking in HCl (10%V/V) for 60 min. The substrates were then rinsed with distilled water for many times to remove the acid.

The ECD preparation was performed as follows [16]: The aqueous $Na_2SeSO_3$ solution (20.0 mL, 0.08 M) was mixed with aqueous solution of $CuSO_4$ (20.0 mL, 0.008 M) and $NH_4Cl$ solution (10 mL, 3.0 M) while bubbling a stream of nitrogen (99.999%) through an inlet. The nitrogen flow was then continued above the solution during deposition to prevent contamination with air. ECD was performed at room temperature using the DC stripping at a constant potential ($-0.6$ V vs. Ag/AgCl) for the glass/FTO electrode. A pre-cleaned platinum sheet was used as a counter electrode. All films prepared by ECD are termed as ECD films. Current vs. time plots during ECD film preparation were measured and showed that the current decreased with time, due to increased cross sectional resistance (across the film) by increasing film thickness. After 15 min deposition, the film thickness was calculated using the Faraday law to be in the range 700—800 nm, assuming the density for copper selenide is 6.0 g/cm$^3$ [29] in accordance with earlier reports [16]. The gravimetrically measured ECD film thickness ($550 \pm 20$ nm) resembled those reported earlier [30,31]. The cross sectional SEM measured thickness was in the range 700—750 nm. The average film sheet resistivity value, measured as described earlier [16], was ~2.5 $\times 10^4$ $\Omega$ cm.

The CBD preparation was performed, as described earlier [31] with amendments, as follows: Solutions of $CuSO_4$ (4.0 mL, 0.5 M), $Na_3C_6H_5O_7$ (4.0 mL, 0.1 M), $Na_2SeSO_3$ (4.0 mL, 0.25 M) were mixed with a few drops of HCl (dilute) and distilled water to make the total solution volume 50 mL and pH ~6.5. The Glass/FTO substrates were dipped inside the solution at room temperature with gentle stirring for different deposition times (2, 4 and 6 h). The CBD films were then taken, rinsed with distilled water and dried. The gravimetrically measured thickness was in the range 40—45 $\mu$m, for films deposited in 2 h. Unless otherwise stated, the films deposited in 2 h were considered in this work as they have better PEC characteristics. The average film sheet resistivity, measured as described earlier [16], was ~1.0 $\times 10^4$ $\Omega$ cm. The choice for deposition time was not arbitrary. Copper selenide films were prepared using similar methods at 60 °C throughout a deposition time of 1 h [31]. In this work CBD deposition at room temperature is intentionally chosen, as described in preparing ECD/CBD film below. Room temperature deposition of CBD films has been reported earlier using a relatively long time of 4 h [22]. In order to optimize

deposition time here, while using room temperature, different deposition times (2, 4 and 6 h) were examined. Depositions in shorter time (1 h or less) were examined at room temperature but yielded films which were difficult to characterize here and were disregarded here.

To prepare ECD/CBD films, the room temperature CBD procedure described above was followed using ECD films in place of the glass/FTO substrates. Room temperature was intentionally used here to avoid affecting the ECD layer (which is originally deposited at room temperature) by any heating. The CBD was continued for 2 h as described above. The gravimetrically measured ECD/CBD film thickness value was in the range 46–52 μm, which is slightly more than the sum of ECD and CBD layer thicknesses separately. The average film sheet resistivity was ~0.8 × $10^4$ Ω cm. The as-prepared film electrodes were used in PEC study here with no annealing. Effect of annealing on film composition, uniformity and PEC characteristics was then investigated afterwards.

Film annealing was performed under a stream of nitrogen gas (99.999%) in a thermostated horizontal tube furnace. The films were placed inside a glass cylinder which was then placed in the furnace after the setting temperature (250 °C) was reached, for 60 min. The resulting films were cooled either by slow cooling (within 3 h) or by fast cooling (in less than 5 min).

### 2.4. The PEC experiment

The copper selenide films were used as working electrodes, and a pre-cleaned platinum sheet was used as a counter and a reference electrode. The PEC experiments were thus conducted in a stoppered two-electrode cell. The internal cell (connected with the counter electrode) was pre-calibrated with Ag/AgCl reference electrode and resembled NHE reference. All PEC results shown here are thus measured with reference to NHE unless otherwise stated. To prevent contamination, nitrogen (99.999%) was bubbled inside the aqueous solution of [$K_3Fe(CN)_6$ (0.1 M)/$K_4Fe(CN)_6$ (0.1 M)/$LiClO_4$(0.1 M)] for 5 min, and the flow was then continued above the solution throughout measurements.

Dark experiments were conducted under a thick black cloth, while photo-experiments were conducted under a solar simulator light (50 W tungsten-halogen lamp). The measured radiation intensity at the electrode surface was AM 38 solar spectrum (~0.002 W/cm$^2$). The low intensity radiation was intentionally chosen to avoid any rise in experimental temperature. For extra precaution, the PEC cell was dipped in a circulated water bath at constant room temperature. Current density vs. potential (J-V) plots were measured vs. NHE, using a PAR 263A Potentiostat-Galvanostat, by dividing the total current (I-V) plots by the exposed electrode area.

Electrode stability was measured using a Polarographic Analyzer (Pol 150) with an MDE 150 stand. Values of short circuit current density ($J_{SC}$) were measured vs. time while keeping the electrode under constant low illumination intensity to avoid cell heating.

## 3. Results and discussions

In this work, three types of copper selenide films were prepared as described above. ECD-CuSe, CBD-CuSe and combined ECD/CBD-CuSe film electrodes were all prepared. The as-prepared three types of films were characterized by different methods and examined in PEC study, with no pre-annealing, for the reasons discussed above. The results are comparatively studied here. The present results are first shown for the as-deposited film electrodes. Effect of annealing on copper selenide film composition, surface uniformity and PEC efficiency is then discussed. The annealing study is restricted to one relatively high temperature (250 °C) just to check if it has any effect

on the electrode PEC performance.

### 3.1. Electronic absorption (EA) spectra

Solid state electronic absorption (EA) spectra were measured for the three copper selenide films, using FTO/Glass sheets for base line correction, as shown in Fig. 1. The EA spectra cannot rule out the possibility of mixed copper selenide phases. The ECD/CBD film spectrum shows better defined absorption band compared to the ECD and CBD films. The Tauc plots were used for better understanding of the spectra, as shown in Fig. 2.

The ECD films were prepared using the optimal conditions (15 min deposition at room temperature) described earlier [16]. Due to its ill-defined EA spectrum, the direct band gap value (2.30 ± 0.20 eV) is difficult to measure accurately by the Tauc method. The CBD film prepared in 2 h showed only slightly smaller band gap value ranging (2.25 ± 0.20 eV). The ECD/CBD film showed a smaller band gap value of 2.20 eV, as shown in Fig. 2. The EA spectra imply that the combined ECD/CBD method yields particles with larger sizes than CBD method, which in turn involves slightly larger particles than the ECD particles. Metal chalcogenide nanoparticles may vary with deposition method [18]. In the nanoscale, larger particles have lower relative surface area and lower numbers of coordinatively unsaturated surface atoms [32,33]. However, the differences in band gap values are too small to give final answer for particle sizes. The difference in band gap value may thus be due to the difference in film thickness, which is known to affect value of band gap for nano-scale particles [34,35]. This confirms the film thickness variations being ECD/CBD > CBD > ECD.

The CuSe films have a wide range of band gap values in literature. In some reports, the value is 2.13 eV [13], while in another report it was much smaller than that [28]. Khomane showed that the band gap value for $Cu_{2-x}Se$ is ~2.2 eV [26], while Liu observed a value of 1.34 eV [36]. Based on literature, CuSe films may have different values depending on method of preparation, particle size, phase purity and other factors. Direct bad gap values in the range 2.0–2.4 eV or higher have been reported [37–39]. All direct band gap values observed here are thus consistent with reported ones for CuSe and $Cu_{2-x}Se$ systems. Considering the value for bulk monocrystalline copper selenide is ~1.05 eV, nano-size particles should exhibit higher band gap values [40].

### 3.2. Photoluminescence (PL) spectra

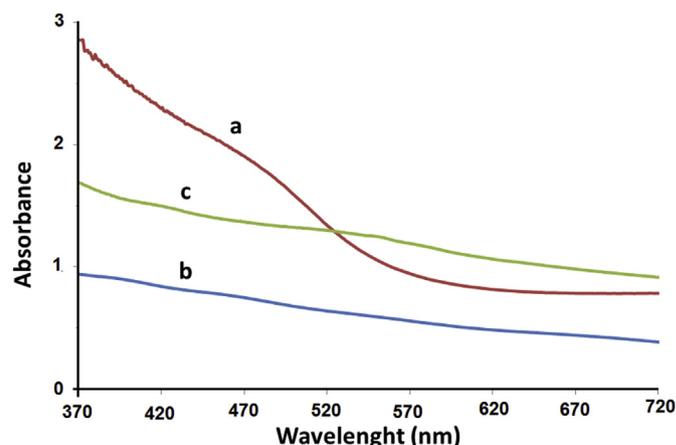Fig. 3 shows the PL emission spectra measured for ECD-, CBD-



**Fig. 1.** Electronic absorption spectra for CBD of the CuSe thin films, deposited in different techniques, a) CBD/ECD, b) CBD and c) ECD.
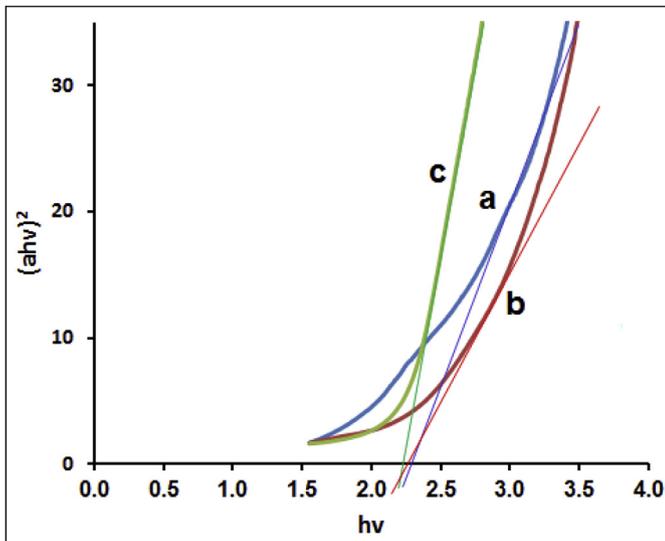
**Fig. 2.** Tauc plots for CuSe films prepared by different methods assuming a direct band gap. a) ECD b) CBD c) ECD/CBD.
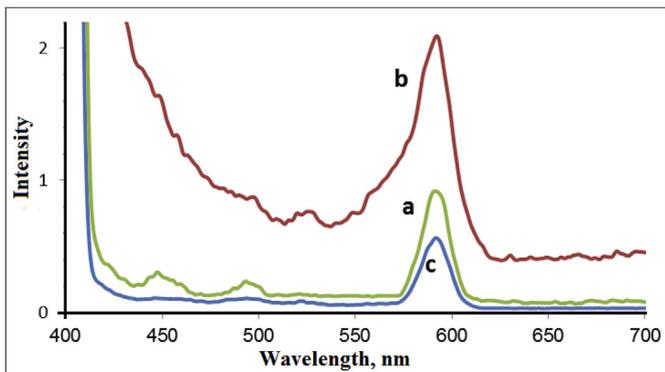


**Fig. 3.** Photoluminescence spectra for CBD of CuSe thin films, deposited by different techniques, a) CBD/ECD, b) CBD, and c) ECD.

and combined ECD/CBD-CuSe films. Due to its lower thickness, the ECD film shows lower emission band intensity than either CBD or ECD/CBD films. The three films show similar emission band wavelengths which makes it difficult to make conclusions about the band gap value differences [40]. Consistent with EA spectra, the PL emission spectra suggest the possibility of the presence of copper selenide, presumably in mixed phases. Further confirmations, for copper selenide presence, are discussed below.

### 3.3. Surface morphology

SEM micrographs for the ECD, CBD and ECD/CBD films are shown in Fig. 4. The Figure shows that different films have different surface morphologies. The ECD/CBD film shows layered structure with flaky agglomerates. The agglomerates involve nano-size particles as described by XRD below. The CBD film resembles that reported for other CBD-CuSe films in its morphology [26,39]. The ECD film micrographs resemble earlier reported ones for ECD prepared films [16] as nano-size particles exist in larger agglomerates with some rod shape.

The AFM shows that the ECD film has higher uniformity and homogeneity than other films, Fig. 5. Fig. 5A and 5B show that the ECD film involves higher interconnection between different particles, than the CBD film, and to a lesser extent the ECD/CBD film. The AFM results confirm the assumption stated above about higher uniformity advantage of ECD films. The profile scanning (Fig. 5C), shows that ~95% of the surface elevations range between 10 and 120 nm. The CBD film has less uniformity (with ~95% elevations in a wide range of 10–200 nm) than the ECD film. ECD/CBD film shows ~95% elevations in the range 75–225 nm. The AFM micrographs for the CBD film resemble those reported earlier [39]. As the EA and PL spectra could not provide a clue to differentiate between different films in terms of band gap values, the surface morphology gives a clue of differences. Among the three different films, the ECD film exhibits highest surface uniformity in terms of narrow profile distribution range (110 nm) and high interconnectivity. The ECD/CBD film shows higher uniformity (with profile distribution range 150 nm) than the CBD film (with profile distribution range 190 nm).

### 3.4. XRD patterns

Fig. 6 shows the XRD patterns for different copper selenide films. The $Cu_{2-x}Se$ characteristic peaks at $2\theta = 26.84°$ (111) and $44.4°$ (220) [41] are observed, but they overlap with other peaks. The former peak overlaps with that for FTO, while the latter also overlaps with that for CuSe which may be present. EDX spectra further confirmed the occurrence of $Cu_{2-x}Se$. The Cu/Se elemental atom ratios for ECD, CBD and ECD/CBD films are 1.01, 1.10 and 1.10 respectively. All films show higher Cu than Se atomic presence, which confirms the presence of $Cu_{2-x}Se$. The lower Cu/Se atom ratio for the ECD indicates the possibility of having higher CuSe phase than in the CBD or ECD/CBD.

The peaks at $2\theta = 27.52°$, and $28.14°$ and $32.00°$, attributed to CuSe hexagonal crystal structure [13,26,28,36,41–44], are observed clearly in the ECD film. The peak at $2\theta = 27.52°$ is not clearly observed in the CBD or ECD/CBD films, which means that the two films do not involve CuSe as a major component. This is consistent with EDX atom ratios discussed above.
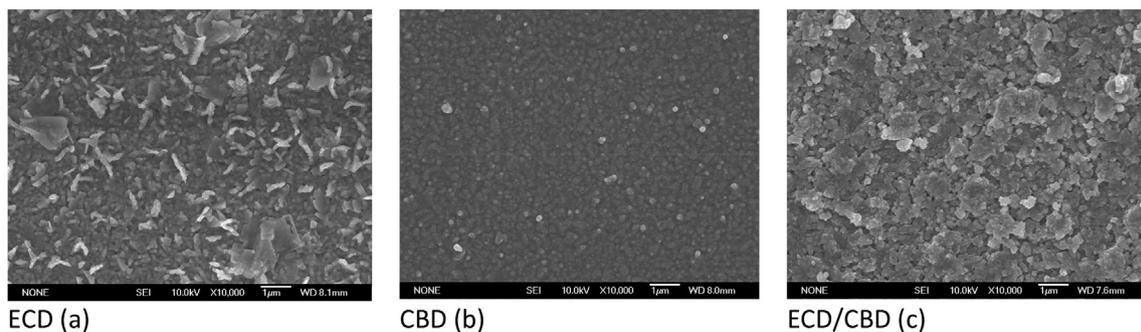


ECD (a)        CBD (b)        ECD/CBD (c)

**Fig. 4.** SEM micrographs for CuSe films prepared by different methods, (a) ECD, (b) CBD and (c) ECD/CBD.
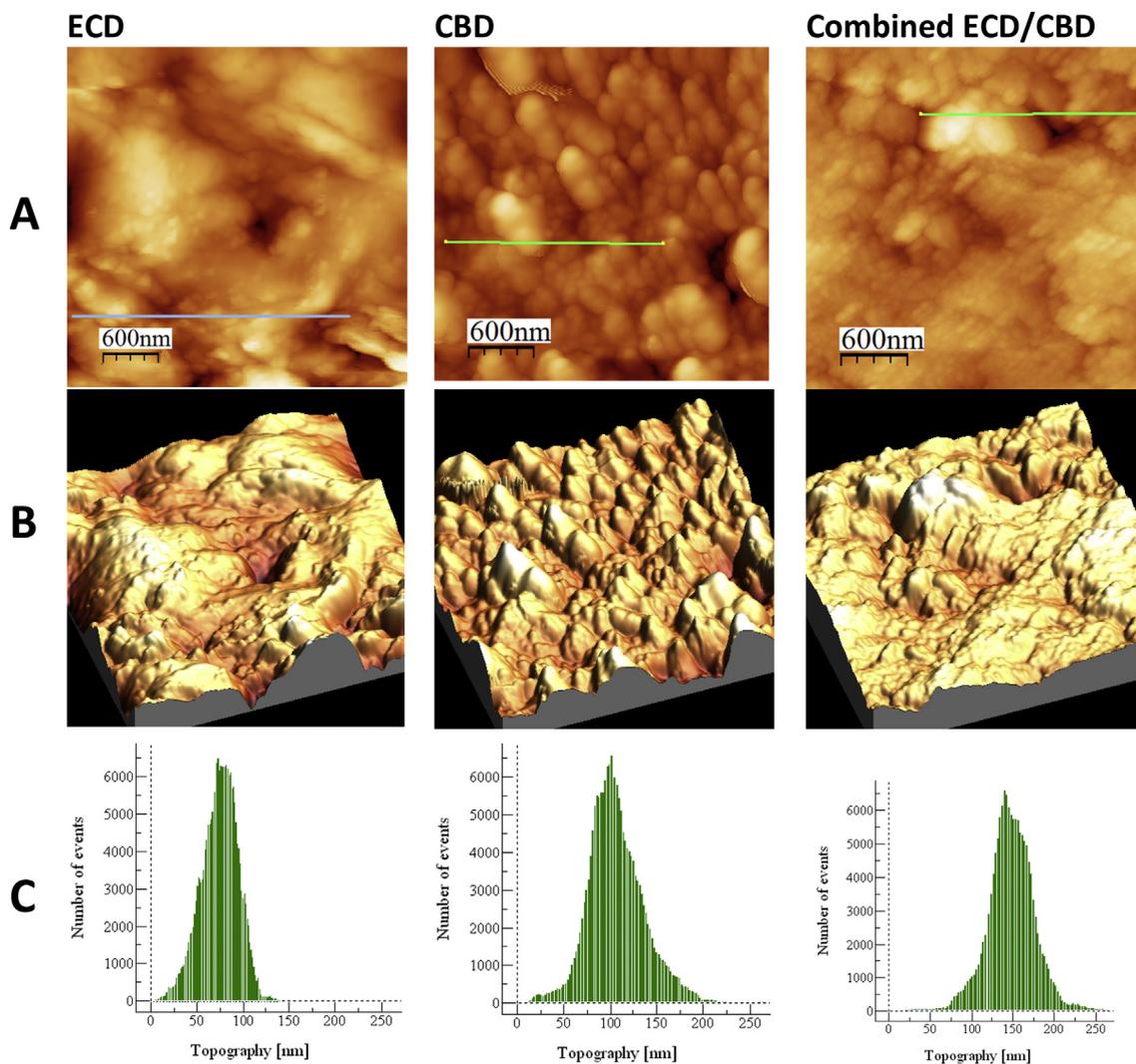
ECD    CBD    Combined ECD/CBD



**Fig. 5.** AFM results for different copper selenide films, (a) 2-dimensional micrographs, (b) 3-dimensional micrographs, and (c) surface topographical distribution.
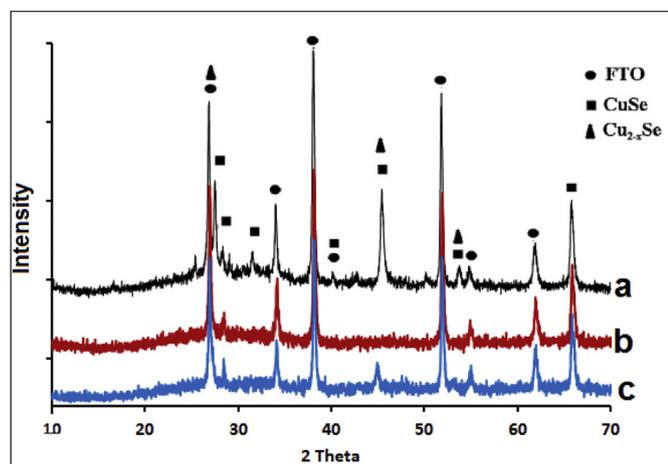


**Fig. 6.** XRD patterns measured for different CuSe film preparations: (a) ECD, (b) CBD and (c) ECD/CBD.

The films do not involve the 29.1° (200) peak characteristic for $CuSe_2$ [41]. Different FTO reflections are also observed in the Figure. The presence of CuO was not evidenced from the XRD patterns, but it should not be totally excluded [37]. The occurrence of CuSe and $Cu_{2-x}Se$ phases, with band gap value ~2.2 eV reported for copper selenide films [26], can thus be justified by the XRD patterns. The XRD patterns clearly show that the materials are polycrystalline.

Calculations based on the Scherrer equation show that the average particle size varies for the films as ECD (25 nm), CBD (30 nm) and ECD/CBD (29 nm). The particle sizes for ECD and CBD films resemble those reported for other CuSe films deposited by different methods [40]. The nano-size particles exist inside larger size agglomerates as explained by SEM and AFM micrographs above. The XRD results confirm the EA and PL spectral results discussed above, as the ECD film involves only slightly smaller particles. No significant effect on the value of the band gap is thus expected.

Based on XRD patterns, EA spectra and PL spectra, no significant differences occur between ECD, CBD and ECD/CBD films in terms of particle sizes or band gap values. Apart from the higher abundance of the CuSe phase in the ECD film, the only noticeable differences between the three films are the surface uniformity, inter-particle connectivity and depth profile variations which are in favor of the ECD film. The oncoming discussions will show how such variations may affect PEC performance of different film electrodes.

## 3.5. PEC study

### 3.5.1. Dark current experiments

Dark current density ($J$) vs. applied potential ($V$) plots were measured for all three ECD, CBD and ECD/CBD film electrodes in aqueous media using the $[Fe(CN)_6]^{4-}/Fe(CN)_6]^{3-}$ redox couple. The redox couple system was chosen based on earlier studies made for ECD-CuSe electrodes [16]. Negative dark current values were observed for all electrodes at negative applied potentials, as shown in Fig. 7. The dark $J$-$V$ plots thus indicate negative values for the onset potential in the dark. The electrode dark $J$-$V$ plots are typical for n-type semiconducting materials. This should be expected due to the presence of $Cu_2Se$ (with $Cu^+$) phase in the films. As per CuSe phase itself, it is known have p-type nature [36]. Therefore, the n-type behavior of the films supports the XRD discussions showing $Cu_{2-x}Se$ (with excess Cu) is a major phase. Similar behaviors have been reported for naked and coated CuSe electrodes with some leakage currents [16]. The Figure shows that the ECD/CBD-CuSe electrode exhibited higher (more negative) onset potential than other counterparts.

### 3.5.2. 2: photo current experiments

Photo $J$-$V$ plots measured for different CuSe film electrodes are shown in Fig. 8. Both ECD and CBD electrodes showed poor short circuit current density ($J_{SC}$) and open circuit potential ($V_{OC}$) values. The ECD/CBD electrode showed higher PEC characteristics than other counterparts.

The Figure shows that all films exhibited n-type nature, as they all showed negative $V_{OC}$ and positive $J_{SC}$ values. Earlier literature shows that CuSe phase has high p-type conductivity with low band gap values [13,26,28,36]. The p-type nature of the CuSe films was explained by Riha [37]. Another study showed that the CuSe electrodes exhibited an n-type behavior as observed from Mott-Schottky plots [45]. Such differences are attributed to the mixed phases in the prepared films, depending on the presence of $Cu^{2+}$ and/or $Cu^+$ ions. The $Cu^+$ ions (in the predominant $Cu_{2-x}Se$ phase) should thus behave as electron donors in the films, which in turn should assume n-type behavior.

The PEC results of the Figure are summarized in Table 1 below. The Table shows low photo-conversion efficiency (PCE, $\eta$%) values for ECD electrode (0.42%) and CBD electrode (1.83%) whereas the
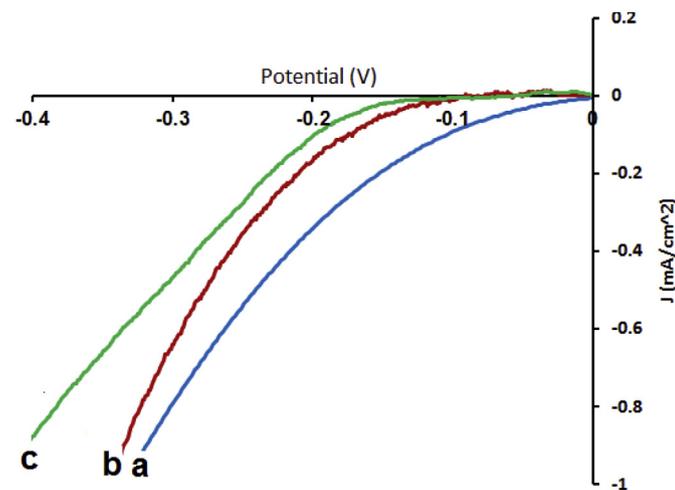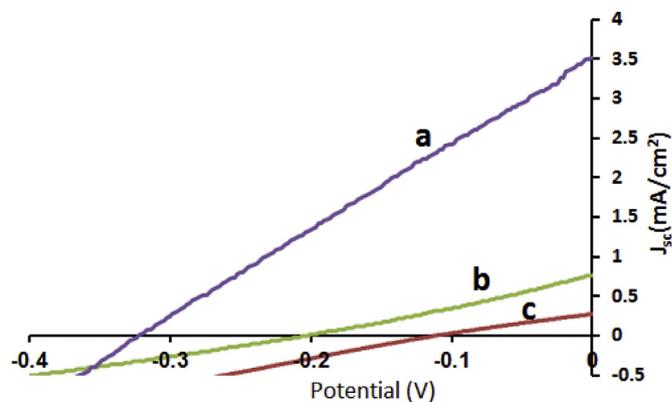


**Fig. 8.** Photo $J$-$V$ plots measured for different CuSe film preparations: (a) ECD/CBD, (b) CBD and (c) ECD. All measurement were made at room temperature using $[Fe(CN)_6]^{4-}/Fe(CN)_6]^{3-}$ redox couple, vs. NHE.

**Table 1**
PEC characteristics measured for different copper selenide film electrodes.

| Entry | Description | $V_{oc}$ (V) | $J_{sc}$ (mA/cm$^2$) | $\eta$%[a] | FF%[b] | Ref. |
|-------|-------------|--------------|----------------------|------------|--------|------|
| A | CBD/ECD (2 h) | −0.32 | 3.52 | 14.6 | 25.41 | This work |
| B | CBD (2 h) | −0.20 | 0.76 | 1.83 | 22.5 | This work |
| C | ECD (15 min) | −0.11 | 0.28 | 0.42 | 26.5 | This work |
| D | ECD (15 min) | −0.18 | 0.12 | 1.04 | 28 | [16] |
| E | CuSe[c] | Small | Small | 0.11 | 28 | [45] |

[a] $\eta$ (%) = [(maximum observed power density)/(reach-in power density)] × 100%.
[b] FF = [(maximum observed power density)/$J_{sc}$ ×$V_{oc}$] × 100%.
[c] All measurement were made at room temperature using $[Fe(CN)_6]^{4-}/Fe(CN)_6]^{3-}$ redox couple, vs. NHE.

ECD/CBD electrode exhibited higher PCE value (14.6%). The low value for the ECD film electrode resembled that observed earlier for ECD-CuSe electrodes [16]. The high abundance of CuSe, besides $Cu_{2-x}Se$ in the ECD film could be a reason. The Table shows also that all electrodes exhibited relatively low fill factor (FF) as reported earlier for CuSe electrodes [16,45]. Despite the enhanced PEC characteristics ($J$-$V$ characteristics and conversion efficiency value) for the ECD/CBD electrode, the FF value is still relatively low. This is known for metal chalcogenide film electrodes. The presence of mixed phases could be a reason for the low FF value in copper selenide film electrodes. Fortunately, the FF value observed here is much higher than those reported earlier for different binary metal chalcogenide film electrodes [10,46]. In order to further improve FF and consequently the conversion efficiency, further modification of the ECD/CBD film electrode should be examined.

The PEC data shown in Table 1 clearly indicate that the ECD/CBD electrode had much higher conversion efficiency than the ECD and the CBD counterparts, studied here or earlier reported. Similar observations were reported for ECD/CBD prepared CdSe [17] and CdS [3] electrodes. In all cases, the ECD/CBD exhibited much higher efficiency than the ECD and the CBD counterparts. Moreover, the ECD/CBD electrode showed conversion efficiency more than 100 fold that other earlier described for CuSe electrodes [45].

Based on the present results, and earlier reports, the preparation method may affect the PEC characteristics of metal chalcogenide film electrodes. The assumption mentioned in Section 1 above works well for CdSe [17], CdS [3] and copper selenide in this work. Successively combining the ECD and CBD preparations together should yield films with preferred properties. The ECD film is assumed to have high uniformity and good adherence with the



**Fig. 7.** Dark $J$-$V$ plots for different CuSe film preparations: (a) ECD, (b) CBD and (c) ECD/CBD.
All measurement were made at room temperature using $[Fe(CN)_6]^{4-}/Fe(CN)_6]^{3-}$ redox couple, vs. NHE.

substrate FTO surface as documented earlier [17,18], which should enhance photocurrent across the copper selenide-FTO interface, as exhibited in Table 1 above. The CBD preparation on the other hand yields thicker films that are more suitable for PEC purposes [20,21]. With a suitable thickness, the semiconductor film electrode can function more effectively in light to electricity conversion. The CBD film thickness was higher than that for the ECD film, which makes it more efficient in PEC processes, as documented for other CdS film electrodes [19,47]. Availability of higher CuSe phase in the ECD film could be another reason for lowering its efficiency compared to the CBD film. The fact that the ECD/CBD shows higher PEC performance is attributed to the poor adherence of the latter film with the substrate surface, as reported earlier [22].

In this work, the ECD exhibits higher uniformity and interparticle connection than CBD, as discussed in Section 3.3 above, which enhances majority carrier mobility. The CBD layer has more suitable thickness which maximizes light absorptivity. The ECD/CBD film electrode thus combines advantages of both ECD and CBD techniques, while avoiding the poor adherence of the copper selenide film to the substrate. To our knowledge, the efficiency value observed from the ECD/CBD-CuSe electrode here (14.6%) has not been preceded for pristine CuSe film electrodes before. The results thus show the added value of combining different preparation methods together in order to prepare highly efficient pristine metal chalcogenide film electrodes.

It should be noted that the PEC enhancement in ECD/CBD film efficiency is not due to the lower sheet resistivity compared to other ECD or CBD counterparts, as described in Section 2.3. That is because in ECD/CBD, the lowering involves the sheet resistivity itself not the cross sectional resistivity.

Further enhancement in the PEC characteristics of the ECD/CBD electrode has been examined. Deposition time for the CBD layer was varied, using 2, 4 and 6 h. Among the different deposition times used, the 2 h time was clearly the best, as discussed above. The maximum efficiency value for the CBD film varied with layer deposition time as: 2 h (1.83%) > 4 h (0.90%) > 6 h (0.40%). With longer deposition times, the CBD film becomes too thick with higher cross sectional resistance. Increased thickness for CBD films prepared from N,N-dimethylselenourea has been documented earlier [28]. Therefore, while using the combined ECD/CBD preparation method, care was taken to use the optimal preparation time 2 h for the CBD layer.

### 3.5.3. Effect of annealing

Effect of pre-annealing the ECD/CBD film electrode on its PEC efficiency was examined. The results show that annealing the electrode at 250 °C or higher lowered its conversion efficiency, as shown in Table 2. Cooling rate also affected the film conversion efficiency. The Table shows efficiency lowering in the order: Non-annealed >> quickly cooled > slowly cooled.

In semi-conductor technology, annealing improves electrode PEC characteristics [16,25], while in some cases, annealing lowers the electrode performance [17]. Copper selenide film electrodes prepared by ECD exhibited efficiency lowering, while those prepared by CBD showed higher efficiency, by annealing at 250 °C [18]. The effect of annealing on ECD/CBD conversion efficiency is

**Table 2**
Effect of annealing (250 °C) and cooling rate on PEC characteristics of ECD/CBD film electrodes.

| Entry | Description | $V_{oc}$ (V) | $J_{sc}$ (mA/cm$^2$) | $\eta$% | FF% |
|---|---|---|---|---|---|
| A | Non-annealed | −0.32 | 3.52 | 14.6 | 25.41 |
| B | Fast cooling | −0.24 | 1.60 | 4.51 | 23.04 |
| C | Slow cooling | −0.07 | 0.82 | 0.76 | 26.02 |

investigated below, in parallel with XRD and EDX results.

Fig. 9 shows the effect of annealing and cooling rate on XRD patterns for ECD/CBD films. In Fig. 9b the especially high and sharp peak at ~ 29.10° is due to the (200) reflection associated with a CuSe$_2$ [10,41,42,44]. The peak is much lower in Fig. 9c, which implies that the peaks in the range 50 - 55° refer to the FTO rather than to CuSe$_2$ in the non-annealed film. In Fig. 9a CuSe$_2$ peaks appear in the quickly annealed film, but to a lesser extent than in Fig. 9b. The occurrence of the CuSe$_2$ (200) peak in case of slowly cooled film is due to the extra allowed time (3 h) for the heated film to undergo phase transition. The presence of CuSe$_2$ phase in the annealed films is one possible reason for lowering PEC performance.

Fig. 9 also shows that the non-annealed ECD/CBD film involves Cu$_{2-x}$Se phase (2ɵ = 26.85°) some CuSe phase (2ɵ = 27.35°). Both ECD and CBD films involve higher CuSe phase than the non-annealed film. This is possibly another reason for the lowering in PEC performance for the annealed films.

EDX spectra, Fig. (S1), further confirm the XRD results. Table 3 summarizes elemental analysis for different film electrodes. The Table shows that the non-annealed ECD/CBD film involves highest atom ratio Cu/Se among the series. The Table also shows that the quickly cooled film has higher Cu/Se atom ratio than the slowly cooled film. In congruence with XRD findings, prolonged exposure to heat in case of slowly cooled film is expected to have higher effect on the film composition. Lowering in Cu$_{2-x}$Se phase by annealing, more obviously in the slow cooling, is one explanation for the negative effect of annealing on PEC performance.

Annealing also affects film crystallinity. Values of XRD relative peak height (with respect to FTO peak at ~38°) for different phases are summarized in Table 4. The non-annealed film has higher Cu$_{2-x}$Se/FTO peak ratio than the annealed films. The CuSe phase is also more available in the annealed films. The peak height ratio for Cu$_{2-x}$S/CuSe in different films varies as: non-annealed > slowly cooled > quickly cooled. The lower amount of the Cu$_{2-x}$Se in the slowly cooled film, compared to the quickly cooled one, is rationalized by the occurrence of CuSe$_2$ phase in the latter, as discussed above. This occurs at the expense of both CuSe and Cu$_{2-x}$Se phases.

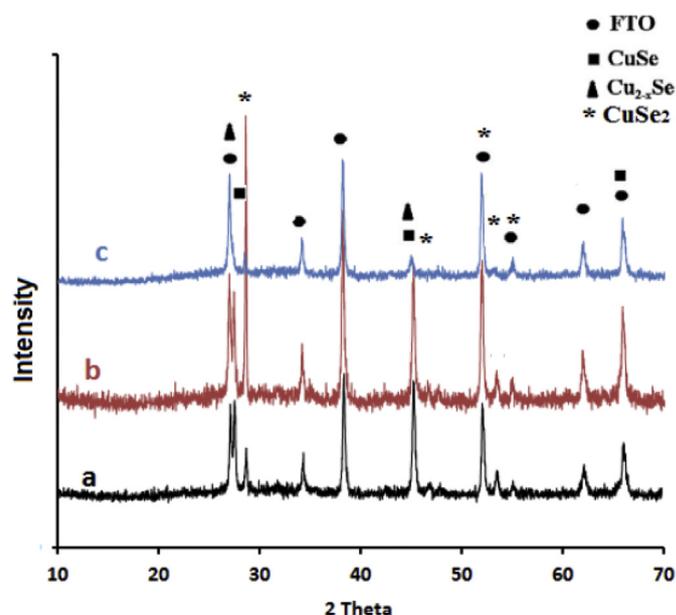The XRD and EDX results indicate that annealing has negative



**Fig. 9.** XRD patterns measured for ECD/CBD-CuSe films: (a) annealed and quickly cooled (b) annealed and slowly Cooled and (c) non-annealed.

**Table 3**
EDX results measured for ECD/CBD films annealed at different temperatures.

| Entry No. | Film description | Cu mass% | Cu atom% | Se mass% | Se atom% | Cu/Se atom ratio |
|---|---|---|---|---|---|---|
| A | Quickly cooled | 16.66 | 11.17 | 19.04 | 10.27 | 1.09 |
| B | Slowly cooled | 22.23 | 17.52 | 33.09 | 20.99 | 0.83 |
| C | Non annealed | 31.71 | 28.21 | 35.88 | 25.68 | 1.10 |

**Table 4**
Effect of annealing on value of XRD relative peak height for ECD/CBD films.

| Entry number | Film description | $Cu_{2-x}Se$ (26.85°)/FTO (~ 38°) peak height ratio | $Cu_{2-x}Se$ (26.85°)/CuSe (27.35°) peak height ratio |
|---|---|---|---|
| A | Annealed & quickly cooled | 0.71 | 2.13 |
| B | Annealed and slowly cooled | 0.59 | 1.15 |
| C | Non-annealed | 0.87 | 2.86 |

effects on the ECD/CBD film crystallinity and composition. Such effects cause lowering in the PEC performance of the copper selenide film electrode, more obviously in case of slow cooling.

For better understanding of the effect of annealing and cooling rate on CuSe film electrode PEC efficiency, the ECD and CBD electrodes were annealed at 250 °C, as shown in Table 5.

For the CBD electrode, efficiency increases by annealing and quick cooling (entries D & E). Slowly cooled CBD film exhibited efficiency lowering compared to non-annealed electrode (entries D & E). The results are consistent with earlier reports, as CuSe films are known to undergo degradation at higher temperatures [28]. The question that comes then is: why does the quickly annealed ECD/CBD film exhibit efficiency lowering, while the quickly annealed CBD film shows enhanced PEC efficiency? For the ECD film electrode, annealing lowers the conversion efficiency in both slow and quick cooling. The lowering in ECD/CBD electrode efficiency is thus attributed to the effect of annealing on the ECD layer.

As the ECD layer, with high uniformity and adherence to FTO surface, becomes more disordered with higher phase mixing, by annealing, the ECD/CBD film electrode should then have lower PEC performance. On the other hand, the as-prepared CBD film is assumed to have high disorder and poor adherence with the FTO surface [22]. Annealing improves inter-particle connection and adherence with the FTO surface in case of CBD electrode, which enhances its PEC conversion efficiency. With slow cooling, excessive exposure to heat has a negative impact on the film electrode as shown in Table 5. Similar behaviors have been reported for ECD- and CBD-CdS electrodes [18].

A closer look at Table 5 shows that quickly cooled ECD/CBD electrode gave higher conversion efficiency values than the slowly cooled counterpart. This is understandable, as the quickly cooled electrodes are exposed to high temperature for only shorter times than the slowly cooled counterparts. With longer exposure to heat, more disorder and more phase mixing occur in slowly cooled films, as described in Table 4. These results are rationalized by the thermal instability of copper selenide films as reported earlier [28,48]. Work is underway here to study effect of annealing the ECD/CBD copper selenide electrode at temperatures below 250 °C, as

described earlier for different materials [16,25]. Effect of coating with electro-active composite materials, is also underway here, to further enhance J-V characteristics, conversion efficiency, stability and fill factor [11,16,25].

### 3.5.4. Electrode stability under PEC conditions

The stability of the ECD, CBD and ECD/CBD film electrodes under PEC conditions was examined under constant light intensity, while using zero bias. Fig. 10 shows that the ECD/CBD electrode exhibit higher $J_{SC}$ values, with time, than other counterparts. The $J_{SC}$ values for both ECD- and CBD-CuSe electrodes do not reach a steady value even after time passes, and continue to decrease with time, which confirms the low stability of the electrodes under PEC conditions. This confirms the assumptions shown above. The ECD/CBD electrode exhibits a steady $J_{SC}$ value (after ~30 min) with continued exposure to light with time, than other electrodes.

The $J_{SC}$ values for ECD/CBD-CuSe electrode in Fig. 10 are lower than those measured for the same electrode in Fig. 8. This is because the stability experiments were performed under lower light intensity (less than 0.0004 W/cm$^2$) than in J-V plot experiments.

The stability plots in the Figure show unsteady $J_{SC}$ values at the beginning. In case of ECD/CBD the values start high and then go down until a steady value is attained after about 30 min. Similar behaviors have been observed for other metal chalcogenide metal electrodes [3,16,18]. The ECD and CBD films exhibit low $J_{SC}$ values at the beginning, which increase to a certain limit and then continue to decrease. This is presumably due to the presence of
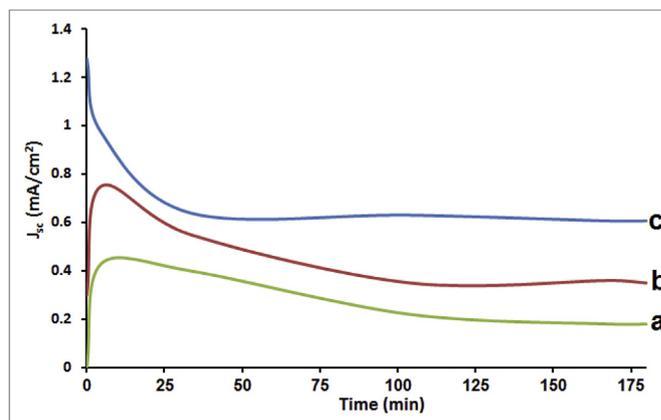
**Table 5**
Effect of annealing on conversion efficiency for ECD and CBD electrodes.

| Entry | Preparation | Description | Efficiency% |
|---|---|---|---|
| A | ECD | Non-annealed | 0.4 |
| B | | Quickly cooled | <0.4 |
| C | | Slowly cooled | <0.4 |
| D | CBD | Non-annealed | 1.83 |
| E | | Quickly cooled | 2.94 |
| F | | Slowly cooled | 0.23 |



**Fig. 10.** Film electrode stability, showing plots of $J_{Sc}$ value vs. time for different CuSe film preparations: (a) ECD, (b) CBD and (c) ECD/CBD. All measurement were made at room temperature using $[Fe(CN)_6]^{4-}/[Fe(CN)_6]^{3-}$ redox couple, vs. NHE.

contaminants at the surface of the electrode. As such contaminants are removed with time, higher $J_{SC}$ occurs. Similar behaviors were reported earlier for metal chalcogenides film electrodes [11,16,18,25]. The continued lowering in $J_{SC}$ for the ECD and CBD film electrodes is attributed to their lower stability to photo-corrosion. The Figure indicates that the ECD/CBD electrode has higher stability than the other counterparts with a steady value for $J_{SC}$ with time. The ECD/CBD film stability is attributed to its higher $J_{SC}$ value, which means faster hole transfer at the solid liquid interface. This prevents hole accumulation in the space charge region, which is responsible for film electrode photo-degradation (instability).

## 4. Conclusion

New copper selenide film electrodes, prepared by electrochemical deposition followed by chemical bath deposition, showed relatively high PEC conversion efficiency values (~14.6%) for te as-prepared film electrode. The new films also showed relatively high stability under PEC conditions. The enhanced PEC characteristics of the new films are attributed to their ability to combine the advantages of both electrochemically deposited and chemical bath deposited film electrodes. The results show how PEC properties of metal chalcogenide film electrodes can be enhanced by simple combined preparation techniques. Annealing at relatively high temperatures affects the film morphology and composition and lowers its PEC characteristics.

## Acknowledgements

## Appendix A. Supplementary data

Supplementary data related to this article can be found at https://doi.org/10.1016/j.solidstatesciences.2017.11.013.

## References

[1] http://www.nrel.gov/ncpv/images/efficiency_chart.jpg.
[2] K. Chopra, P. Paulson, V. Dutta, Thin-film solar cells: an overview, Prog. Photovoltaics Res. Appl. 12 (2004) 69—92.
[3] A. Zyoud, I. Saadeddin, S. Khurduj, M.M. Mari'e, Z.M. Hawash, M.I. Faroun, G. Campet, D. Park, H.S. Hilal, Combined electrochemical/chemical bath depositions to prepare CdS film electrodes with enhanced PEC characteristics, J. Electroanal. Chem. 707 (2013) 117—121.
[4] N. Sabli, Z.A. Talib, W.M.M. Yunus, Z. Zainal, H.S. Hilal, M. Fujii, SnSe Thin film electrodes prepared by vacuum evaporation: enhancement of photoelectrochemical efficiency by argon gas condensation method, Electrochemistry 82 (2014) 25—30.
[5] B.M. Palve, V.S. Kadam, C.V. Jagtap, S.R. Jadkar, H.M. Pathan, A simple chemical route to synthesis the CuSe and CuS counter electrodes for titanium oxide

[6] based quantum dot solar cells, J. Mater. Sci. Mater. Electron. 28 (2017) 14394—14401.
[6] S. Thirumavalavan, K. Mani, S. Suresh, Structural, surface morphology, optical and electrical investigation of cdse thin films, Chalcogenide Lett. 12 (2015) 237—246.
[7] F. Liu, J. Zhu, L. Hu, B. Zhang, J. Yao, M.K. Nazeeruddin, M. Grätzel, S. Dai, Low-temperature, solution-deposited metal chalcogenide films as highly efficient counter electrodes for sensitized solar cells, J. Mater. Chem. A 3 (2015) 6315—6323.
[8] G.W. Mudd, III-VI Metal Chalcogenide Semiconductor Nanosheets and Heterostructures, in, Ph.D. Thesis, University of Nottingham, 2016.
[9] C. Han, Synthesis of Nanostructured Metal Chalcogenides Used for Energy Conversion and Storage, 2015.
[10] S.M. Ho, Metal chalcogenide thin films for photoelectrochemical cell applications: a Review, Middle-East J. Sci. Res. 24 (2016) 1232—1235.
[11] H. Sabri, S. Saleh, A. Zyoud, N.N. Abdel-Rahman, I. Saadeddin, G. Campet, D. Park, M. Faroun, H.S. Hilal, Enhancement of CdSe film electrode PEC characteristics by metalloporphyrin/polysiloxane matrices, Electrochimica Acta 136 (2014) 138—145.
[12] K. Tyagi, B. Gahtori, S. Bathula, S. Auluck, A. Dhar, Band structure and transport studies of copper selenide: an efficient thermoelectric material, Appl. Phys. Lett. 105 (2014) 173905.
[13] J. Montes-Monsalve, R.B. Correa, A.P. Mora, Optical and structural study of CuSe and CuSe/in thin films, J. Phys. Conf. Ser. (2014), 012024. IOP Publishing.
[14] M.A. Contreras, L.M. Mansfield, B. Egaas, J. Li, M. Romero, R. Noufi, E. Rudiger-Voigt, W. Mannstadt, Improved energy conversion efficiency in wide bandgap Cu (In, Ga) Se 2 solar cells, in: Photovoltaic Specialists Conference (PVSC), 2011 37th IEEE, IEEE, 2011, pp. 000026—000031.
[15] J.J. Scragg, P.J. Dale, D. Colombara, L.M. Peter, Thermodynamic aspects of the synthesis of thin-film materials for solar cells, ChemPhysChem 13 (2012) 3035—3046.
[16] A. Zyoud, R.S. Al-Kerm, R.S. Al-Kerm, M. Waseem, H.H. Mohammed, D. Park, G. Campet, N. Sabli, H.S. Hilal, High PEC conversion efficiencies from CuSe film electrodes modified with metalloporphyrin/polyethylene matrices, Electrochimica Acta 174 (2015) 472—479.
[17] A. Zyoud, N.N. Abdul-Rahman, G. Campet, D. Park, H. Kwon, T.W. Kim, H.-J. Choi, M.H. Helal, H.S. Hilal, Enhanced PEC characteristics for CdSe polycrystalline film electrodes prepared by combined electrochemical/chemical bath depositions, J. Electroanal. Chem. 774 (2016) 7—13.
[18] A. Zyoud, I. Saa'deddin, S. Khudruj, Z.M. Hawash, D. Park, G. Campet, H.S. Hilal, CdS/FTO thin film electrodes deposited by chemical bath deposition and by electrochemical deposition: a comparative assessment of photoelectrochemical characteristics, Solid State Sci. 18 (2013) 83—90.
[19] S. Pawar, L. Deshmukh, Thickness dependent properties of electro-chemical-photovoltaic (ecpv) cells formed with chemically deposited CdS films, Bull. Mater. Sci. 7 (1985) 127—130.
[20] H.S. Hilal, R.M. Ismail, A. El-Hamouz, A. Zyoud, I. Saadeddin, Effect of cooling rate of pre-annealed CdS thin film electrodes prepared by chemical bath deposition: enhancement of photoelectrochemical characteristics, Electrochimica Acta 54 (2009) 3433—3440.
[21] A. Zyoud, N. Zaatar, I. Saadeddin, M.H. Helal, G. Campet, M. Hakim, D. Park, H.S. Hilal, Alternative natural dyes in water purification: anthocyanin as TiO2-sensitizer in methyl orange photo-degradation, Solid State Sci. 13 (2011) 1268—1275.
[22] B. Durdu, U. Alver, A. Kucukonder, Ö. Söğüt, M. Kavgaci, Investigation on zinc selenide and copper selenide thin films produced by chemical bath deposition, Acta Phys. Pol. A 124 (2013) 41—45.
[23] M. Barote, A. Yadav, E. Masumdar, Synthesis, characterization and photoelectrochemical properties of n-CdS thin films, Phys. B Condens. Matter 406 (2011) 1865—1871.
[24] R. Pandey, S. Mishra, S. Tiwari, P. Sahu, B. Chandra, Comparative study of performance of CdTe, CdSe and CdS thin films-based photoelectrochemical solar cells, Sol. Energy Mater. Sol. Cells 60 (2000) 59—72.
[25] A. Zyoud, R.S. AlKerm, R.S. Alkerm, D. Park, M.H. Helal, G. Campet, R.W. Muthaffar, H. Kwon, H.S. Hilal, Enhanced PEC characteristics of pre-annealed CuS film electrodes by metalloporphyrin/polymer matrices, Sol. Energy Mater. Sol. Cells 144 (2016) 429—437.
[26] A. Khomane, Synthesis and characterization of chemically deposited Cu2-xSe thin films, Archives Appl. Sci. Res. 4 (2012) 1857—1863.
[27] I. Ezenwa, N. Okereke, L. Okoli, Optical properties of copper selenide thin films, Int. Res. J. Eng. Sci. Technol. Innovation 2 (2013) 82—87.
[28] C.A. Estrada, P. Nair, M. Nair, R.A. Zingaro, E.A. Meyers, Chemical bath deposition of ZnSe and CuSe thin films using N, N-Dimethylselenourea, J. Electrochem. Soc. 141 (1994) 802—806.
[29] http://www.guidechem.com/dictionary/en/1317-41-5.html.
[30] K. Ramesh, S. Thanikaikarasan, B. Bharathi, Structural, morphological and optical properties of copper selenide thin films, Int. J. ChemTech Res. 6 (2014) 5408—5411.
[31] B. Pejova, I. Grozdanov, Chemical deposition and characterization of Cu3Se2 and CuSe thin films, J. Solid State Chem. 158 (2001) 49—54.
[32] B. Avinash, V. Chathurmukha, C. Naveen, M. Rajeeva, H. Jayanna, A.R. Lamani, Influence of particle size on band gap and dielectric properties of TiO2 nanomaterials, in: International Conference on Condensed Matter and Applied Physics (ICC 2015): Proceeding of International Conference on Condensed Matter and Applied Physics, AIP Publishing, 2016, 020347.

[33] D. Segets, J.M. Lucas, R.N. Klupp Taylor, M. Scheele, H. Zheng, A.P. Alivisatos, W. Peukert, Determination of the quantum dot band gap dependence on particle size from optical absorbance and transmission electron microscopy measurements, Acs Nano 6 (2012) 9021–9032.

[34] N. Das, P. Ghosh, M. Mitra, K. Chattopadhyay, Effect of film thickness on the energy band gap of nanocrystalline CdS thin films analyzed by spectroscopic ellipsometry, Phys. E Low-dimensional Syst. Nanostructures 42 (2010) 2097–2102.

[35] J.-P. Xu, R.-J. Zhang, Y. Zhang, Z.-Y. Wang, L. Chen, Q.-H. Huang, H.-L. Lu, S.-Y. Wang, Y.-X. Zheng, L.-Y. Chen, The thickness-dependent band gap and defect features of ultrathin ZrO 2 films studied by spectroscopic ellipsometry, Phys. Chem. Chem. Phys. 18 (2016) 3316–3321.

[36] Y.-Q. Liu, F.-X. Wang, Y. Xiao, H.-D. Peng, H.-J. Zhong, Z.-H. Liu, G.-B. Pan, Facile microwave-assisted synthesis of klockmannite CuSe nanosheets and their exceptional electrical properties, Sci. Rep. 4 (2014).

[37] S.C. Riha, D.C. Johnson, A.L. Prieto, Cu2Se nanoparticles with tunable electronic properties due to a controlled solid-state phase transition driven by copper oxidation and cationic conduction, J. Am. Chem. Soc. 133 (2010) 1383–1390.

[38] R.S. Mane, A.V. Shaikh, O.-S. Joo, S.-H. Han, H.M. Pathan, Electrodeposition of copper selenide films from acidic bath and their properties, in: Indian Vacuum Society Symposium on Thin Films: Science and Technology, AIP Publishing, 2012, pp. 194–196.

[39] S. Thirumavalavan, K. Mani, S. Sagadevan, Investigation of the structural, optical and electrical properties of copper selenide thin films, Mater. Res. 18 (2015) 1000–1007.

[40] M.A. Malik, P. O'Brien, N. Revaprasadu, A novel route for the preparation of CuSe and CuInSe 2 nanoparticles, Adv. Mater. 11 (1999) 1441–1444.

[41] M.-Z. Xue, Y.-N. Zhou, B. Zhang, L. Yu, H. Zhang, Z.-W. Fu, Fabrication and electrochemical characterization of copper selenide thin films by pulsed laser deposition, J. Electrochem. Soc. 153 (2006) A2262–A2268.

[42] Syed Ghause Ibrahim, Ashish V. Kadu, Physical and optical properties of chemically deposited copper selenide (CuSe) thin films at room temperature, Int. J. Innovative Res. Sci. Eng. Technol. 6 (2017) 365–368.

[43] V. Milman, B. Winkler, J.A. White, C.J. Pickard, M.C. Payne, E.V. Akhmatskaya, R.H. Nobes, Electronic structure, properties, and phase stability of inorganic crystals: a pseudopotential plane-wave study, Int. J. Quantum Chem. 77 (2000) 895–910.

[44] K.-S. Kim, H.-C. Jeong, J.-Y. Cho, D.-H. Kang, H.-K. Kim, H.-M. Yoo, I.-W. Shim, Preparation of copper (Cu) thin films by MOCVD and their conversion to copper selenide (CuSe) thin films through selenium vapor deposition, Bull. Korean Chem. Soc. 24 (2003) 647–649.

[45] K. Rathod, Synthesis, Characterization and Applications of Mixed Chalcogenide Thin Films, Ph.D. Thesis, Aurangabad University, 2015.

[46] P.D. Matthews, P.D. McNaughter, D.J. Lewis, P. O'Brien, Shining a light on transition metal chalcogenides for sustainable photovoltaics, Chem. Sci. 8 (2017) 4177–4187.

[47] J. Ximello-Quiebras, G. Contreras-Puente, J. Aguilar-Hernandez, G. Santana-Rodriguez, A.A.-C. Readigos, Physical properties of chemical bath deposited CdS thin films, Sol. Energy Mater. Sol. Cells 82 (2004) 263–268.

[48] S.D. Kang, J.-H. Pöhls, U. Aydemir, P. Qiu, C.C. Stoumpos, R. Hanus, M.A. White, X. Shi, L. Chen, M.G. Kanatzidis, Enhanced stability and thermoelectric figure-of-merit in copper selenide by lithium doping, Mater. Today Phys. 1 (2017) 7–13.